



Article

PEI-Functionalized Carbon Nanotube Thin Film Sensor for CO₂ Gas Detection at Room Temperature

Maeum Han ¹, Soonyoung Jung ^{1,2}, Yeonsu Lee ^{1,2}, Daewoong Jung ^{2,*} and Seong Ho Kong ^{1,*}

¹ School of Electronic and Electrical Engineering, Kyungpook National University, Daegu 41566, Korea; mehan@knu.ac.kr (M.H.); sallmen@kitech.re.kr (S.J.); yeonsu2629@kitech.re.kr (Y.L.)

² Advanced Mechatronics R&D Group, Korea Institute of Industrial Technology (KITECH), Yeongcheon 38822, Korea

* Correspondence: dwjung@kitech.re.kr (D.J.); shkong@knu.ac.kr (S.H.K.)

Abstract: In this study, a polyethyleneimine (PEI)-functionalized carbon nanotube (CNT) sensor was fabricated for carbon dioxide detection at room temperature. Uniform CNT thin films prepared using a filtration method were used as resistive networks. PEI, which contains amino groups, can effectively react with CO₂ gas by forming carbamates at room temperatures. The morphology of the sensor was observed, and the properties were analyzed by scanning electron microscope (SEM), Raman spectroscopy, and fourier transform infrared (FT-IR) spectroscopy. When exposed to CO₂ gas, the fabricated sensor exhibited better sensitivity than the pristine CNT sensor at room temperature. Both the repeatability and selectivity of the sensor were studied.

Keywords: carbon dioxide; carbon nanotube; gas sensor



Citation: Han, M.; Jung, S.; Lee, Y.; Jung, D.; Kong, S.H. PEI-Functionalized Carbon Nanotube Thin Film Sensor for CO₂ Gas Detection at Room Temperature. *Micromachines* **2021**, *12*, 1053. <https://doi.org/10.3390/mi12091053>

Academic Editor: Niall Tait

Received: 21 July 2021

Accepted: 30 August 2021

Published: 30 August 2021

Publisher's Note: MDPI stays neutral with regard to jurisdictional claims in published maps and institutional affiliations.



Copyright: © 2021 by the authors. Licensee MDPI, Basel, Switzerland. This article is an open access article distributed under the terms and conditions of the Creative Commons Attribution (CC BY) license (<https://creativecommons.org/licenses/by/4.0/>).

1. Introduction

Carbon dioxide is a colorless and odorless gas, contributing to the greenhouse effect; it is a major cause of global warming [1–4]. Hence, reliable and low-cost CO₂ gas sensing is of great significance. Since CO₂ is an unreactive gas, operating gas sensors at room temperature is challenging [5,6]. Diverse sensing principles and/or materials for detecting CO₂ gas have been reported, including nondispersive infrared (NDIR), metal oxides, polymers, and nanomaterials. Each has their own strengths and weaknesses. Most common sensors are NDIR sensors and metal oxide sensors; however, IR sensors have disadvantages such as bulkiness of transducers and high power consumption during operation [7–10]. Metal oxide gas sensors typically work at temperatures higher than 200 °C, which increases the difficulty of manufacturing and requires high power consumption [11–13]. In contrast, polymer-based sensors do not share these disadvantages. Polymer-based sensors are polymer films that can broadly detect and identify various components in the air to target analyte [14]. A coating of organic detecting layers is easy to synthesize and improves gas detection. In addition, a polymer is easily processable and can be coated using various coating methods such as drop casting and spin coating [15–17]. However, polymer receptor layers also are burdened by significant drawbacks, some of which are rapid aging and low resistance to sensor poisoning.

Recently, CNTs have proven to be promising candidates for gas sensitive materials owing to their large effective surface area and abundant sites for adsorbing gas molecules, as well as their hollow geometry, chemical properties, and high aspect ratio. Surface area can promote the physical adsorption or chemical reaction with target gas molecules and efficient and rapid signal conversion [18,19]. The sensing mechanism is based on the transfer of electrons to chemical analytes through charge transfer between the CNTs and gas molecules. As evidenced by experiments involving electron-donating (NH₃) and electron-withdrawing molecules (NO₂), the sensing mechanism can still operate where electrons are transferred when interacting with different analytes [20,21].

CNT sensors are sensitive to charge donors and acceptors but not to Lewis acids or bases such as CO₂ gas [22]. Sensitivity can be improved using a recognition layer that triggers a chemical reaction that alters the properties of the CNT sensor. Although the chemical functionalization of CNTs for the sensor has been explored, the disadvantage of covalent modification is that it destroys the physical properties of CNTs, resulting in a loss of conductance [23–26]. We performed a noncovalent functionalization of CNTs by applying an amine-rich polyethyleneimine (PEI) polymer. PEI contains primary, secondary, and tertiary amine groups; hence, it can easily adsorb CO₂ at room temperature [27]. The fundamental mechanism is the interaction between the amino groups with CO₂ at room temperature to form carbamates by physisorption and reversible reaction between CNTs and CO₂ gas [28].

CNT sensors can be fabricated using various methods, including direct growth, screen-printing, electrophoresis, and spraying [29–32]. However, these manufacturing methods are difficult to reproduce, and the sensitivity of the sensors produced will be low. In comparison, CNT thin films prepared using the filtration method can make a dense CNT network. The procedures are simple, including dispersion and filtration of the CNT solution, making them suitable for practical applications. A dense arrangement of CNTs is expected to exhibit higher sensitivity and repeatability. In addition, a CNT thin film with a paper-like appearance is suitable for flexible and conductive applications such as flexible devices [33].

In this study, PEI-functionalized CNT thin film sensors were fabricated for CO₂ gas detection at room temperature. A highly uniform CNT thin film was used as a resistive network for gas sensing. PEI functionalization was implemented to enhance the CO₂ capture capability of amino groups. The sensor was characterized through SEM, Raman spectroscopy, and FT-IR, and its responses to different concentrations of CO₂ gas were studied. In addition, the fabricated sensor was evaluated in terms of its repeatability, selectivity, and flexibility. The results can stimulate research on flexible and wearable gas-sensing systems.

2. Materials and Methods

2.1. Polyethyleneimine (PEI)-Functionalized Carbon Nanotube (CNT) Thin Film Sensor

We fabricated a CNT thin film using MWCNTs (Sigma-Aldrich, St. Louis, MO, USA), the average length and diameter of which were in the ranges of 6–13 nm and 2.5–20 µm, respectively. MWCNTs and methanol were mixed in the ratio of 0.2 g per 100 mL, added with 0.5 wt % PEI (Sigma-Aldrich), and the mixture was stirred for 12 h. Thereafter, the mixture was homogenized for 1 h using ultrasonic equipment. After fully dispersed, a vacuum filtration process was conducted with 8 µm filter paper (Whatman, Marlborough, MA, USA). After drying the CNT thin film by heating at 70 °C for 1 h, it was placed on a polyimide substrate to make a silver electrode with a gap of approximately 2 cm at both ends of the sample. Subsequently, the silver electrode was heated at 90 °C for 15 min and dried to fabricate a gas sensor. Figure 1 shows the image of the filtration production system, the fabricated sensor, and the flexibility of the sensor.

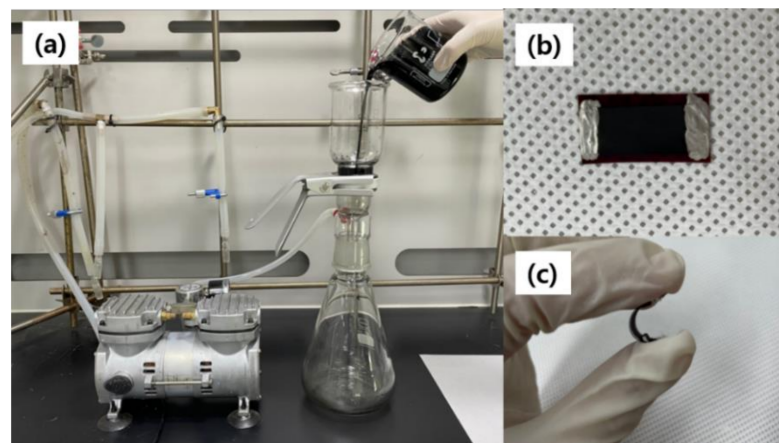


Figure 1. (a) Filtration system; (b) the image of the fabricated sensor; (c) the flexibility of the sensor.

2.2. Gas Sensor Measurement

The gas response of the sensor was measured in a gas chamber at room temperature. The CO₂ and nitrogen gases (Korea Nano Gas Inc., Hae Song Industry Co., Dongan-gu, Anyang-si, Gyeonggi-do, Korea) were used as target and carrier gases, respectively. During the experiments, the gas concentration was controlled using a mass flow controller (MFC). The total gas flow rate was set to 500 sccm. We used nitrogen gas instead of air as the carrier gas to eliminate the influence of moisture and oxygen in the air. The resistance of the fabricated sensors was sampled while a constant 5 V DC voltage was applied.

3. Results and Discussion

3.1. Morphology of PEI-Functionalized CNT Thin Film

The morphology of the PEI-functionalized CNT film was studied using SEM. A CNT film is essentially a porous structure composed of randomly entangled CNTs. The filtration method can ensure the uniformity of CNT deposition. The CNT film has a relatively smooth surface, and the roughness ranges from a few hundred nanometers to microns [34].

Figure 2 shows the morphologies of the pristine and PEI-functionalized CNTs. The diameters of the pristine and PEI-functionalized CNT films are approximately 10 and 16 nm, respectively. As shown in Figure 2b, individual CNTs were wrapped by penetrated PEI into the CNT film, observing the thicker diameter. In addition, the EDS spectrum of the PEI-functionalized CNT emitters exhibited signatures of nitrogen. Because PEI has one nitrogen in every three atoms in the backbone, nitrogen signatures in the PEI-functionalized CNT emitter signifies the presence of PEI at the surface of the CNT [27]. The SEM image shows that PEI was successfully introduced onto the CNTs.

On the other hand, the thickness of PEI-functionalized CNT film is rather decreased from 60 to 13.5 μm after functionalization of PEI. The outer surface of the CNTs is covered and penetrated by PEI agglomerates because of the viscosity characteristic of the PEI. The PEI and CNT are expected to aggregate and cause a thin thickness of the CNT films.

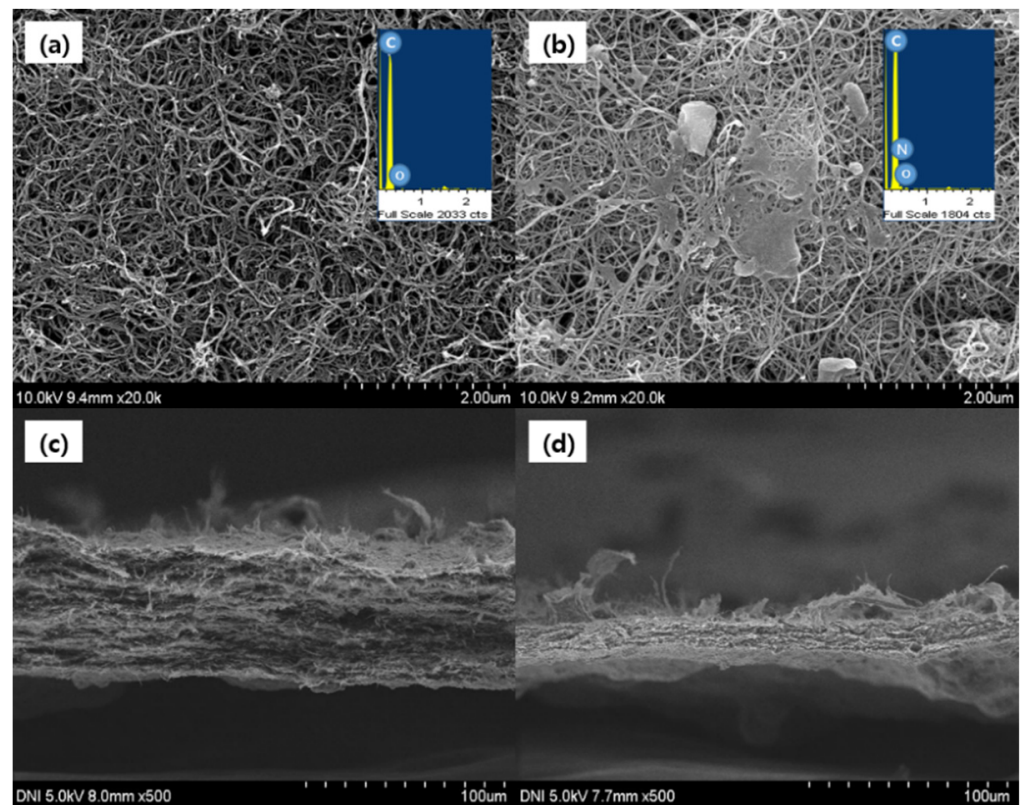


Figure 2. Scanning electron microscope (SEM) images of the top view of (a) pristine carbon nanotube (CNT); (b) polyethyleneimine (PEI)-functionalized CNT; the side view of (c) pristine CNT; (d) PEI-functionalized CNT.

3.2. Raman Analysis of PEI-Functionalized CNT Thin Film

Raman spectroscopy is an effective method for characterizing carbon-based nano-materials. The fabricated sensor was characterized under a laser power of 10 mW and laser excitation of 532 nm. The effect before and after PEI functionalization of the CNTs was confirmed through Raman spectral observation. Figure 3 shows the Raman spectra measured on raw and PEI-functionalized CNT films. The peaks centered at 1326 and 1571 cm^{-1} represent the D and G peaks of the CNTs, respectively. The shape of the D peak is related to the defect structure of the CNT, and the G band corresponds to the graphite in the lattice. The ratio between the intensities of the D and G bands is denoted by I_D/I_G value and indicates the degree of CNT defect.

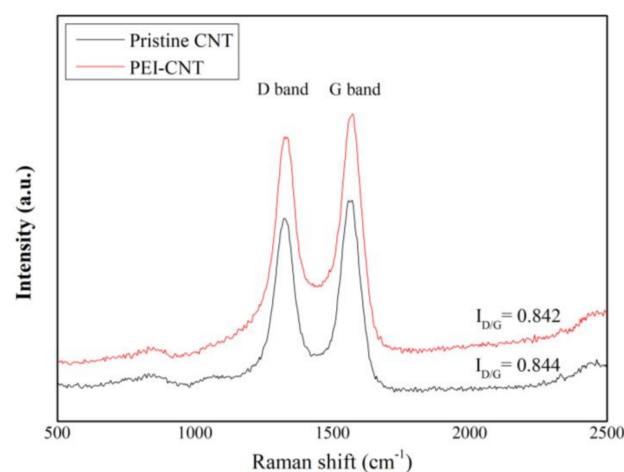


Figure 3. Raman spectroscopy comparison of pristine CNT and PEI-functionalized CNT.

As shown in Figure 3, the I_D/I_G values of pristine CNT and PEI-functionalized CNT are similar, which are about 0.842 and 0.844, respectively. These results indicate that PEI functionalization does not significantly damage the CNT structure. For the pristine CNT, the G band was observed at 1571 cm^{-1} , but for PEI-functionalized CNT, the G-band showed blue shifted to 1574 cm^{-1} . Lu et al. explained that this phenomenon was caused by that the lone pair electrons of N atoms in chains interact π -electrons of CNT. Therefore, the electron density of CNT was strengthened, and polarization of CNT was increased due to the p- π conjugation of the CNT [35,36].

3.3. Fourier Transform Infrared (FT-IR) Analysis of PEI-Functionalized CNT Thin Film

FT-IR analysis was carried out the analysis of PEI-functionalized CNTs in comparison with the pristine CNTs. Figure 4 shows the FT-IR spectra of the pristine and PEI-functionalized CNTs. The organic moieties of PEI clearly appear themselves in the region at $2800\text{--}3000\text{ cm}^{-1}$ (C-H stretching) in contrast with pristine CNTs. In addition, a new band at 3401 cm^{-1} (N-H stretching) appears, and the band at 1382 cm^{-1} and 1072 cm^{-1} also correspond to the C-N stretching vibration due to the PEI [37,38]. From the results, it can be confirmed that the amine group was successfully introduced on the surface of the CNT thin film.

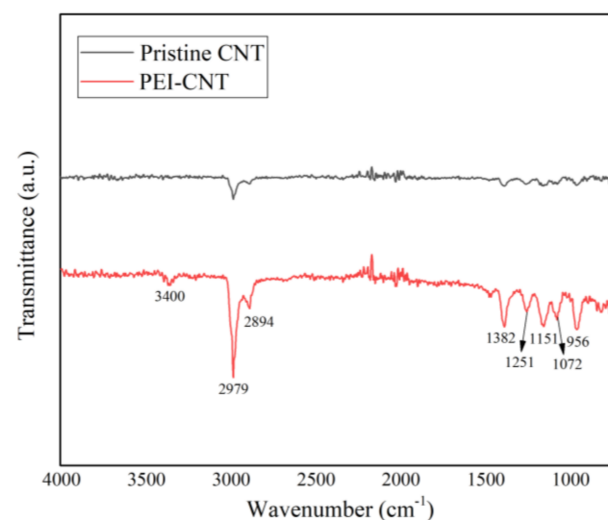


Figure 4. Fourier transform infrared (FT-IR) spectroscopy comparison of pristine CNT and PEI-functionalized CNT.

3.4. Sensor Responses

The adsorption/desorption of gas molecules has a significant effect on the electrical properties of CNTs. It has been reported that the CO_2 gas sensing of pristine CNTs is low because of the weak interaction between CO_2 molecules and the CNT surface [22]. However, it has been found that the sensitivity of CNTs to CO_2 gas can be significantly increased through surface functionalization [39,40]. To confirm the CO_2 gas-sensing properties of CNTs, both pristine and functionalized CNT sensors were fabricated, and gas-sensing experiments were conducted.

To evaluate its response to CO_2 gas, the sensor was placed in a chamber, and the flow rate of the mixed gas was set to 500 sccm. The sensitivity to the CO_2 concentration was measured and determined using the following equation:

$$\text{Response (\%)} = \frac{(R - R_0)}{R_0} \times 100, \quad (1)$$

where R is the change in the resistance of the sensor after gas injection, and R_0 is the resistance of the gas sensor before the reaction. Figure 5 shows the gas-sensing characteristics of

the pristine and PEI-functionalized CNT sensors. When the sensor was exposed to CO₂ gas, the electrical resistance of the PEI-functionalized CNT sensor increased with the increase in the CO₂ gas concentration.

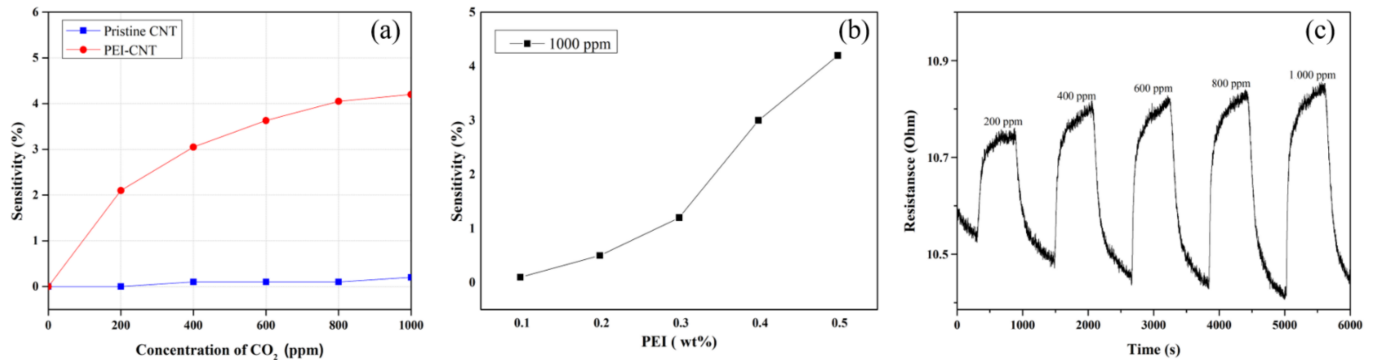


Figure 5. The sensitivities of (a) pristine- and PEI-CNT sensors; (b) different ratio of PEI; (c) the CNT sensor to the concentration of CO₂ gas from 200 to 1000 ppm.

Typically, CO₂ is a nonreactive molecule, but it combines with an amine group to form a carbamate. This combination can be explained based on the hard soft acids bases (HSAB) theory. The HSAB theory can explain the direct interaction between the CO₂ molecules and the amino group-based polymer. Hard Lewis acids tend to bind hard Lewis bases, and soft Lewis acids tend to bind soft Lewis bases. Since CO₂ is a hard acid, it can interact with the primary amines in PEI, which are a hard base. PEI is a highly branched polymer with primary, secondary, and tertiary amino groups. At room temperature, the reaction of an amino group with CO₂ is reversible, forming carbonate [41].

According to the HSAB theory, the test results are appropriate. In addition, PEI exhibits n-type properties because of the electron-donating properties of the NH₂ group in PEI [5,22]. The reaction between the CO₂ molecule and PEI forms carbamates, which reduce the overall electron-donating effect of PEI. Thus, the PEI exhibits properties consistent with electron removal from the sensor. The high density of the amine functional groups in PEI is associated with significant n-doping to the point where there is an adverse effect of p-doping [42]. Therefore, the electrical resistance of the fabricated sensor showed a characteristic that increased with the introduction of CO₂ gas. Figure 5 shows the CO₂ gas sensitivity, different ratio of PEI, and response time of pure and PEI-functionalized CNTs. The CO₂ gas concentration was measured while varying it from 200 to 1000 ppm. As shown in Figure 5a, the reactivity of pure CNTs to CO₂ gas at room temperature is low; however, the PEI-functionalized CNT sensor exhibits a greater reactivity to CO₂ gas. After the CO₂ gas was injected into the chamber, the resistance of the sensor increased rapidly until it stabilized, and the resistance change increased linearly with increasing CO₂ gas concentration. When the CO₂ gas injection was stopped and only nitrogen was injected into the chamber, the resistance of the sensor returned to its initial value. Moreover, higher sensitivity was observed in the CNT sensor with a large amount of PEI, as shown in Figure 5b. A larger PEI:CNT ratio can provide more active sites for adsorbed CO₂ gas. This result was in line with above sensing mechanism. Subsequent experiments were conducted using a sample with 0.5 wt % of PEI.

The response time T_a was defined as the time required for the change in the resistance to reach 90% of the equilibrium value after injecting the target gas, and the recovery time T_b was defined as the time required for the sensor to return to the initial 10%. The sensor was exposed to CO₂ gas until near saturation was reached, the CO₂ injection was stopped, and the sensor was desorbed by injecting only nitrogen gas until the resistance returned to its initial value. Figure 5c shows that the response and recovery times of the sensor are the same, i.e., approximately 10 min. After adsorbing the CO₂ molecules, the PEI acted as a mediator between the CNTs and CO₂ gas, facilitating charge transfer. Because of the

interaction between PEI and the adsorbed molecules during desorption, electrons can be effectively removed from the CNTs without the use of an external source, such as external heating. Moreover, because of the dense CNT thin film structure, it enables stable electron transport to the electrode when measuring the resistance.

To evaluate the actual ability of the sensor to operate, the comparison experiments were conducted in dry air as carrier gas instead of nitrogen gas and different relative humidity (RH) values. As shown in Figure 6a, the sensitivity of the PEI-functionalized CNT sensor is reduced under dry air environmental conditions. The degraded performance in dry air is due to the fact that a compensation of n-doping effect by reacting oxygen (O_2) gas in dry air with PEI on CNT films [42]. On the other hand, upon exposure of the PEI-functionalized CNT sensor in humid nitrogen gas, the sensitivity remarkably increased, reaching an increase of 2 times at 1000 ppm of CO_2 in 80% RH, as shown Figure 6b. These results are same as those of previous studies [43,44]. Son et al. reported that the charge transfer between PEI and CNTs plays an important role in the improvement of sensitivity under wet conditions. They proposed that the functionalization of PEI on CNT generated the n-doping effect, which encourages the donation of electrons from the protonated polymer, leaving the water molecules in the humidity to act as a source of protons. Once CO_2 gas was introduced to the sensor, the charge movements occurred between the amino group in the PEI and the CO_2 gas to result in an acid–base equilibrium state, supporting the formation of carbamates and bicarbonates [43]. Yoon et al. also explained that the exposure to CO_2 gas under a humidified atmosphere generates amidinium bicarbonates, which produce an increase in the density of mobile hole carriers in the polymer chain, which in turn increases the overall conductance of the sensor and leads to a response [44].

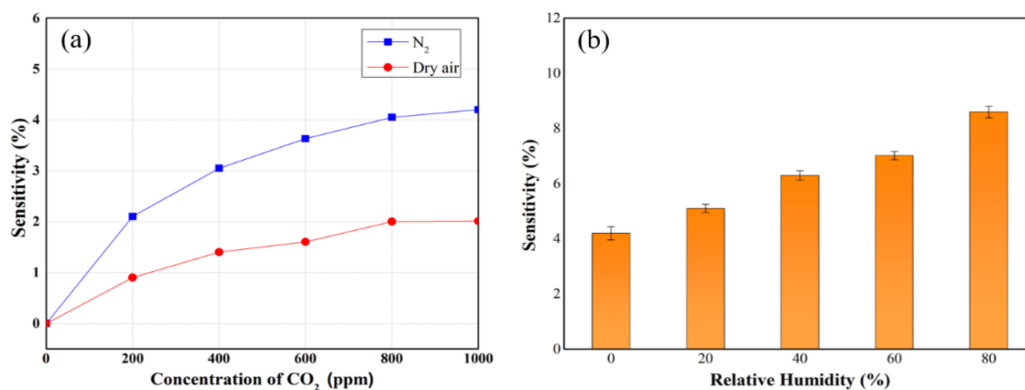


Figure 6. The sensitivities of PEI-functionalized CNT sensors under (a) nitrogen and dry air; (b) different humidity level.

To confirm the repeatability and stability of the sensor, five CO_2 gas response characteristics and long-term experiments were performed. As shown in Figure 7a, a stable and reversible reaction characteristic can be observed in several repeated experiments, with negligible hysteresis. As described above, the CNT thin film prepared using the filtration method is constituted by stacking a large number of dense individual CNTs. Because of the strong van der Waals force and large contact area between the stacked CNTs, the stability was high even after repeated experiments, which prevented damage. In comparison, in the case of printed or spray-based CNT sensors, the low density of individual CNTs and weak interactions result in structural damage after repeated experiments, thereby deteriorating the sensor properties [45]. In terms of repeatability, the experiment was performed five times with a CO_2 gas concentration of 600 ppm, a gas adsorption time of 10 min, and a desorption time of 10 min, with all the cycles lasting 20 min. The results showed that the CO_2 gas detection characteristics have good reproducibility and stability as shown Figure 7b.

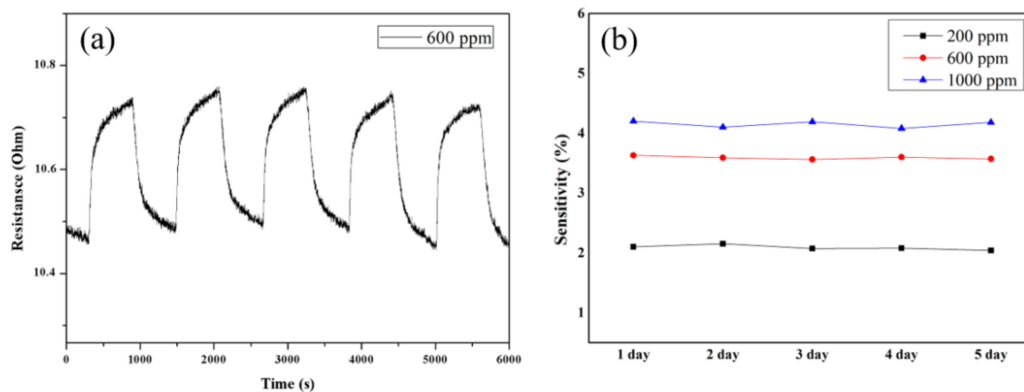


Figure 7. The (a) repeatability and (b) stability of PEI-functionalized CNT sensor.

The selectivity of the sensor for a specific gas is an important characteristics of the sensor. Selectivity is the capability of a sensor to measure only one gas species relative to other gases. Typically, CNTs react with other gases such as NH_3 and NO_2 at room temperature [46,47]. Therefore, it is particularly important to improve the CNT-based CO_2 gas selectivity of the sensor for commercialization. Figure 8 shows the sensitivity of the PEI-functionalized CNT gas sensor to different gases. The sensitivity to CO_2 gas is highest (4.2%) at 1000 ppm. O_2 gas reacted slightly with the sensor, but PEI interacted more strongly with the CO_2 gas at room temperature; thus, the reaction value was much lower than that of the CO_2 gas.

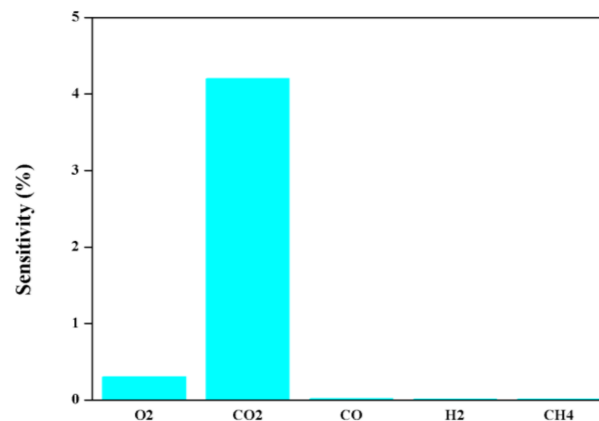


Figure 8. The selectivity of PEI-functionalized CNT toward various gases.

With the growing demand for wearable and flexible device products, the demand for flexible sensors is increasing. These flexible sensors require properties that are flexible but not volatile with respect to sensitivity and shape. However, in the case of a metal or metal oxide-based sensor, it is difficult to fabricate a flexible sensor, but in the case of a sensor using a CNT thin film, a high flexibility can be obtained [48].

To evaluate the flexibility of the fabricated sensor, the sensor was fabricated on a polyimide film, bent and unfolded several times in a cylinder with a radius of 8 mm, and then the sensitivity characteristics based on the CO_2 gas concentration were evaluated. After the bending test, no change in the shape of the sensor was observed, and it was confirmed that the resistance was largely the same. Figure 9 shows the sensitivity results with respect to the CO_2 gas concentration before and after bending. The fabricated sensor has structural stability and flexibility owing to the very high density of the CNT film, and its applicability to wearables and portable devices was confirmed.

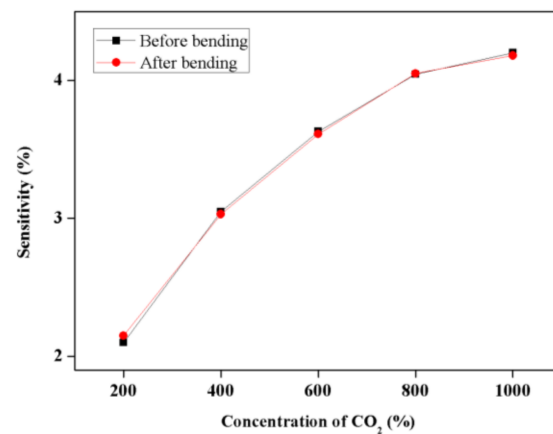


Figure 9. The sensitivity of PEI-functionalized CNT before and after bending tests.

The Table 1 shows a comparison of the sensing properties of reported CO₂ sensors. The PEI-functionalized CNT sensor was successfully created for sensitive, responsive, and flexible measurement of CO₂ over a wide concentration range at room temperature.

Table 1. Comparison of the sensing properties of CO₂ sensors.

Materials	Type of Sensor	Gas Concentration (ppm)	Sensitivity ($\Delta R/R$)	Operating Temperature ($^{\circ}\text{C}$)	Flexibility	Reference
ZnO	Chemiresistor	200–1025	2.3	250	-	[49]
Porous silicon/ α -MoO ₃	Chemiresistor	50–150	15	250	-	[50]
PEDOT-BPEI	Chemiresistor	1000	2.7	Room tem.	-	[51]
PIL-Al ₂ O ₃	Chemiresistor	150–2400	1.7	Room tem.	-	[52]
CNT	Chemiresistor	50–800	2.25	Room tem.	Flexible	[53]
PEI-CNT	Chemiresistor	200–1000	4.2	Room tem.	Flexible	This work

4. Conclusions

In summary, a PEI-functionalized CNT sensor was fabricated for CO₂ gas detection at room temperature. A PEI-functionalized CNT thin film was fabricated using the filtration method. The response performance of the sensor to CO₂ gas at room temperature was investigated. The sensor was found to exhibit better sensing characteristics than the pristine CNT sensor because of the acid–base interaction between the amine groups in PEI and CO₂ gas molecules. The proposed sensor shows characteristics such as good sensitivity, repeatability, and selectivity. In addition, the sensor exhibits good flexibility owing to the high density of the CNT film. These results confirm its potential for wearable and portable CO₂ devices.

Author Contributions: Conceptualization, M.H. and S.J.; software, Y.L. and S.J.; validation, M.H. and S.J.; formal analysis, M.H. and S.H.K.; investigation, Y.L. and S.J.; data curation, M.H. and S.J.; writing—original draft preparation, M.H.; writing—review and editing, D.J. All authors have read and agreed to the published version of the manuscript.

Funding: This study was supported by the BK21 FOUR project funded by the Ministry of Education, Korea (4199990113966). This work was supported by a Korea Innovation Foundation (INNOPOLIS) grant funded by the Korea government (MSIT) (2020-DD-UP-0348). This study was conducted with the support of the Korea Institute of Industrial Technology.

Data Availability Statement: The data presented in this study are available on request from the corresponding author.

Acknowledgments: We are grateful for technical assistance from the staff members at KNU and KITECH.

Conflicts of Interest: The authors declare no conflict of interest.

References

1. Kim, C.; Getz, P.; Kim, M.G.; Brand, O. Room temperature CO₂ sensing based on interdigitated capacitors and resonant cantilevers. In Proceedings of the 2017 19th International Conference on Solid-State Sensors, Actuators and Microsystems (TRANSDUCERS), Kaohsiung, Taiwan, 18–22 June 2017; pp. 1532–1535.
2. Wang, H.; Vagin, S.I.; Rieger, B.; Meldrum, A. An ultrasensitive fluorescent paper-based CO₂ sensor. *ACS Appl. Mater. Interfaces* **2020**, *12*, 20507–20513. [[CrossRef](#)]
3. Zhang, J.; Liu, X.; Neri, G.; Pinna, N. Nanostructured materials for room temperature gas sensors. *Adv. Mater.* **2015**, *28*, 795–831. [[CrossRef](#)] [[PubMed](#)]
4. Huang, L.; Zhang, Z.; Li, Z.; Chen, B.; Ma, X.; Dong, I. Multifunctional graphene sensors for magnetic and hydrogen detection. *ACS Appl. Mater. Interfaces* **2015**, *7*, 9581–9588. [[CrossRef](#)]
5. Zhou, Y.; Jiang, Y.; Xie, G.; Wu, M.; Tai, H. Gas sensors for CO₂ detection based on RGO-PEI films at room temperature. *Chin. Sci. Bull.* **2014**, *59*, 1999–2005. [[CrossRef](#)]
6. Fine, G.F.; Cavanagh, L.M.; Afonja, A.; Binions, R. Metal oxide semi-conductor gas sensors in environmental monitoring. *Sensors* **2010**, *10*, 5469–5502. [[CrossRef](#)] [[PubMed](#)]
7. Smulko, J.M. New approaches for improving selectivity and sensitivity of resistive gas sensors: A review. *Sens. Rev.* **2015**, *35*, 340–347. [[CrossRef](#)]
8. Ji, H.; Zeng, W.; Li, Y. Gas sensing mechanisms of metal oxide semiconductors: A focus review. *Nanoscale* **2019**, *11*, 22664–22684. [[CrossRef](#)]
9. Hanafi, R.; Mayasari, R.D.; Raharjo, J.; Nuryadi, R. Electrochemical sensor for environmental monitoring system: A review. *AIP Conf. Proc.* **2019**, *2169*, 030007.
10. Fang, Q.; Chetwynd, D.G.; Covington, J.A.; Toh, C.S.; Gardner, J.W. Micro-gas-sensor with conducting polymers. *Sens. Actuators B Chem.* **2002**, *84*, 66–71. [[CrossRef](#)]
11. Shin, W.S.; Young, S.J.; Ji, L.W.; Water, W.; Meen, T.H.; Shiu, H.W. Effect of oxygen plasma treatment on characteristics of TiO₂ photodetectors. *IEEE Sens. J.* **2011**, *11*, 3031–3035.
12. Young, S.J. Photoconductive gain and noise properties of ZnO nanorods schottky barrier photodiodes. *IEEE J. Sel. Top. Quantum Electron.* **2014**, *20*, 3801204.
13. Rout, C.S.; Hegde, M.; Rao, C. H₂S sensors based on tungsten oxide nanostructures. *Sens. Actuators B Chem.* **2008**, *128*, 488–493. [[CrossRef](#)]
14. Reethirajan, S.; Jayas, D.S.; Sadistap, S. Carbon dioxide sensors for the agri-food industry—A review. *Food Bioprocess Technol.* **2009**, *2*, 115–121. [[CrossRef](#)]
15. Tian, K.; Gerald, F.; Elfed, L.; Wang, X.; Liang, H.; Wang, P. A high sensitivity temperature sensor based on balloon-shaped bent SMF structure with its original polymer coating. *Meas. Sci. Technol.* **2018**, *29*, 085104. [[CrossRef](#)]
16. Tan, Y.; Peng, H.; Liang, C.; Yao, S. A new assay system for phenacetin using biomimic bulk acoustic wave sensor with a molecularly imprinted polymer coating. *Sens. Actuators B Chem.* **2001**, *73*, 179–184. [[CrossRef](#)]
17. Zee, F.; Judy, J. Micromachined polymer-based chemical gas sensor array. *Sens. Actuators B Chem.* **2001**, *72*, 120–128. [[CrossRef](#)]
18. Afrin, R.; Shah, N.A. Room temperature gas sensors based on carboxyl and thiol functionalized carbon nanotubes buckypapers. *Diam. Relat. Mater.* **2015**, *60*, 42–49. [[CrossRef](#)]
19. DeGraff, J.; Liang, R.; Le, M.Q.; Capsal, J.; Ganet, F.; Cottinet, P. Printable low-cost and flexible carbon nanotube buckypaper motion sensors. *Mater. Des.* **2017**, *133*, 47–53. [[CrossRef](#)]
20. Misewich, J.A.; Martel, R.; Avouris, P.H.; Tsang, J.C.; Heinze, S.; Tersoff, J. Electrically Induced Optical Emission from a carbon nanotube FET. *Science* **2003**, *300*, 783–786. [[CrossRef](#)]
21. Kong, J.; Franklin, N.; Zhou, C.; Chapline, M.; Peng, S.; Cho, K.; Dai, H. Nanotube Molecular Wires as Chemical Sensors. *Science* **2000**, *287*, 622–625. [[CrossRef](#)]
22. Star, A.; Han, T.; Joshi, V.; Gabriel, J.; Gruner, G. Nanoelectronic Carbon Dioxide sensors. *Adv. Mater.* **2004**, *22*, 2049–2052. [[CrossRef](#)]
23. Hirsch, A. Functionalization of single-walled carbon nanotubes. *Angew. Chem. Int. Ed.* **2002**, *41*, 1853–1859. [[CrossRef](#)]
24. Sun, Y.-P.; Fu, K.; Lin, Y.; Huang, W. Functionalized carbon nanotubes: Properties and applications. *Acc. Chem. Res.* **2002**, *35*, 1096–1104. [[CrossRef](#)]
25. Tasis, D.; Tagmatarchis, N.; Georgakilas, V.; Prato, M. Soluble Carbon Nanotubes. *Chem. Eur. J.* **2003**, *9*, 4000–4008. [[CrossRef](#)] [[PubMed](#)]
26. Banerjee, S.; Kahn, M.G.C.; Wong, S.S. Rational Chemical Strategies for Carbon Nanotube Functionalization. *Chem. Eur. J.* **2003**, *9*, 1898–1908. [[CrossRef](#)]
27. Satyapal, S.; Filburn, T.; Trela, J.; Strange, J. Performance and Properties of a Solid Amine Sorbent for Carbon Dioxide Removal in Space Life Support Applications. *Energy Fuels* **2001**, *15*, 250–255. [[CrossRef](#)]
28. Dell'Amico, D.B.; Calderazzo, F.; Labella, L.; Marchetti, F.; Pampaloni, G. Converting Carbon Dioxide into Carbamate Derivatives. *Chem. Rev.* **2003**, *103*, 3857–3898. [[CrossRef](#)]
29. Zhanga, H.; Liua, Y.; Kuwataa, M.; Bilottiab, E.; Peijs, T. Improved fracture toughness and integrated damage sensing capability by spray coated CNTs on carbon fibre prepreg. *Compos. Part A* **2015**, *70*, 102–110. [[CrossRef](#)]

30. Fennimore, A.; Cheng, L.; Roach, D. stable under-gate triode CNT field emitter fabricated via screen printing. *Diam. Relat. Mater.* **2008**, *17*, 2005–2009. [[CrossRef](#)]
31. Lee, S.; Lee, D.; Yu, H.; Campbell, E.; Park, Y. Production of individual suspended single-walled carbon nanotubes using the ac electrophoresis technique. *Appl. Phys. A* **2004**, *78*, 283–286. [[CrossRef](#)]
32. Dikonimos Makris, T.; Giorgi, L.; Giorgi, R.; Lisi, N.; Salernitano, E. CNT growth on alumina supported nickel catalyst by thermal CVD. *Diam. Relat. Mater.* **2005**, *14*, 815–819. [[CrossRef](#)]
33. Lu, S.; Chen, D.; Wang, X.; Shao, J.; Ma, K.; Zhang, L.; Araby, S.; Meng, Q. Real-time cure behaviour monitoring of polymer composites using a highly flexible and sensitive CNT buckypaper sensor. *Compos. Sci. Technol.* **2017**, *152*, 181–189. [[CrossRef](#)]
34. Rein, M.D.; Breuer, O.; Wagner, H.D. Sensors and sensitivity: Carbon nanotube buckypaper films as strain sensing devices. *Colloid Surf. B-Biointerfaces* **2017**, *160*, 493–499. [[CrossRef](#)]
35. Lu, H.; Hang, A.; Zhang, Y.; Ding, L.; Zheng, Y. The effect of polymer polarity on the microwave absorbing properties of MWNTs. *RSC Adv.* **2015**, *5*, 64925–64931. [[CrossRef](#)]
36. Zhao, Q.; Daniel Wagner, H. Raman spectroscopy of carbon–nanotube–based composites. *Phil. Trans. R. Soc. Lond. A* **2004**, *362*, 2407–2424. [[CrossRef](#)]
37. Zaaeri, F.; Khoobi, M.; Rouini, M.; Akbari Javar, H. pH-responsive polymer in a core–shell magnetic structure as an efficient carrier for delivery of doxorubicin to tumor cells. *Int. J. Polym. Mater. Polym. Biomater.* **2018**, *67*, 967–977. [[CrossRef](#)]
38. Li, K.; Zhang, C.; Du, Z.; Li, H.; Zou, W. Preparation of humidity-responsive antistatic carbon nanotube/PEI nanocomposites. *Synth. Met.* **2012**, *162*, 2010–2015. [[CrossRef](#)]
39. Wang, Y.; Zhang, K.; Zou, J.; Wang, X.; Sun, L.; Wang, T.; Zhang, Q. Functionalized horizontally aligned CNT array and random CNT network for CO₂ sensing. *Carbon* **2017**, *117*, 263–270. [[CrossRef](#)]
40. Siefker, Z.A.; Boyina, A.; Braun, J.E.; Zhao, X.; Boudouris, B.W.; Bajaj, N.; Chiu, G.; Rhoads, J. A Chemiresistive CO₂ Sensor Based on CNT-Functional Polymer Composite Films. *IEEE Sens.* **2020**. [[CrossRef](#)]
41. Sun, B.; Xie, G.; Jiang, Y.; Li, X. Comparative CO₂-sensing Characteristic studies of PEI and PEI/Starch Thin Film Sensors. *Energy Procedia* **2011**, *12*, 726–732. [[CrossRef](#)]
42. Shim, M.; Javey, A.; Wong, N.; Kam, S.; Dai, H. Polymer Functionalization for Air-Stable n-Type Carbon Nanotube Field-Effect Transistors. *J. Am. Chem. Soc.* **2001**, *123*, 11512–11513. [[CrossRef](#)] [[PubMed](#)]
43. Son, M.; Pak, Y.; Chee, S.; Auxilia, F.M.; Kim, K.; Lee, B.; Lee, S.; Kang, S.K.; Lee, C.; Lee, J.S.; et al. Charge transfer in graphene/polymer interfaces for CO₂ detection. *Nano Res.* **2018**, *11*, 3529–3536. [[CrossRef](#)]
44. Yoon, B.; Choi, S.J.; Swager, T.M.; Walsh, G.F. Switchable single-walled carbon nanotube–polymer composites for CO₂ sensing. *ACS Appl. Mater. Interfaces* **2018**, *10*, 33373–33379. [[CrossRef](#)]
45. Han, M.; Kim, J.; Kang, S.; Jung, D. Post-treatment effects on the gas sensing performance of carbon nanotube sheet. *Appl. Surf. Sci.* **2019**, *481*, 597–603. [[CrossRef](#)]
46. Xial, Z.; Kong, L.B.; Ruan, S.; Li, X.; Yu, S.; Li, X.; Jiang, Y.; Yao, Z.; Ye, S.; Wang, C.; et al. Recent development in nanocarbon materials for gas sensor applications. *Sens. Actuator B. Chem.* **2018**, *274*, 235–267.
47. Wang, Y.; Yeow, J.T.W. A review of carbon nanotube-based gas sensor. *J. Sens.* **2009**, *2009*, 493904. [[CrossRef](#)]
48. Park, S.; Kim, J.; Chu, M.; Khine, M. Highly Flexible Wrinkled Carbon Nanotube Thin Film Strain Sensor to Monitor Human Movement. *Adv. Mater. Technol.* **2016**, *1*, 1600053. [[CrossRef](#)]
49. Kanaparthi, S.; Singh, S.G. Chemiresistive sensor based on zinc oxide nanoflakes for CO₂ detection. *ACS Appl. Nano Mater.* **2019**, *2*, 700–706. [[CrossRef](#)]
50. Thomas, T.; Kumar, Y.; Ramón, J.A.R.; Agarwal, V.; Guzmán, S.S.; Reshmi, R.; Sanal, K.C. Porous silicon/ α -MoO₃ nanohybrid based fast and highly sensitive CO₂ gas sensors. *Vacuum* **2021**, *184*, 109983. [[CrossRef](#)]
51. Chiang, C.J.; Tsai, K.T.; Lee, Y.H.; Lin, H.W.; Yang, Y.L.; Shih, C.C.; Dai, C.A. In situ fabrication of conducting polymer composite film as a chemical resistive CO₂ gas sensor. *Microelectron. Eng.* **2013**, *111*, 409–415. [[CrossRef](#)]
52. Willa, C.; Schmid, A.; Briand, D.; Yuan, J.; Koziej, D. Lightweight, Room-Temperature CO₂ Gas Sensor Based on Rare-Earth Metal-Free Composites An Impedance Study. *ACS Appl. Mater. Interfaces* **2017**, *9*, 25553–25558. [[CrossRef](#)] [[PubMed](#)]
53. Lin, Z.D.; Young, S.J.; Chang, S.J. CO₂ gas sensors based on carbon nanotube thin films using a simple transfer method on flexible substrate. *IEEE Sens. J.* **2015**, *15*, 7017–7020. [[CrossRef](#)]